Quantification of Cell Response to Polymeric Composites Using a Two-Dimensional Gradient Platform

Nancy J. Lin[*,1], Haiqing Hu[2], Lipin Sung[2] and Sheng Lin-Gibson[*,1]

[1]*Polymers Division, National Institute of Standards and Technology, Gaithersburg, MD 20899-8543, USA*

[2]*Materials and Construction Research Division, National Institute of Standards and Technology, Gaithersburg, MD 20899-8615, USA*

Abstract: A simple and straightforward screening process to assess the toxicity and corresponding cell response of dental composites would be useful prior to extensive *in vitro* or *in vivo* characterization. To this end, gradient composite samples were prepared with variations in filler content/type and in degree of conversion (DC). The DC was determined using near infrared spectroscopy (NIR), and the surface morphology was evaluated by laser scanning confocal microscopy (LSCM). RAW 264.7 macrophage-like cells were cultured directly on the composite gradient samples, and cell viability, density, and area were measured at 24 h. All three measures of cell response varied as a function of material properties. For instance, compositions with higher filler content had no reduction in cell viability or cell density, even at low conversions of 52%, whereas significant decreases in viability and density were present when the filler content was 35% or below (by mass). The overall results demonstrate the complexity of the cell-material interactions, with properties including DC, filler type, filler mass ratio, and surface morphology influencing the cell response. The combinatorial approach described herein enables simultaneous screening of multiple compositions and material properties, providing a more thorough characterization of cell response for the improved selection of biocompatible composite formulations and processing conditions.

Keywords: Biocompatibility, cell spreading, cell viability, combinatorial, dental composites, degree of conversion, surface roughness, cell-material interaction.

INTRODUCTION

Polymeric composites have steadily gained a broader acceptance as dental restorative materials largely due to their superior aesthetics [1]. Most dental composites are comprised of a photopolymerizable dimethacrylate matrix reinforced with filler particles. Although several properties have improved over the past few years, particularly with respect to strength and wear resistance, many other properties critical to clinical longevity remain less than optimal [2]. In addition to efforts focused on improving various physical and mechanical properties, there exists a renewed interest in the biocompatibility of this class of materials [3-5]. An appropriate biological response for a given application is essential for successful clinical use of new and existing dental materials. Materials with poor biocompatibility may result in toxicity, mutagenicity, sensitization, inflammation, and a loss of pulp vitality [6], and often lead to restoration failure and replacement. Many of the deleterious biological effects of dental materials are due to the leaching of various chemical species. In addition, dental materials can also affect tissues in the oral and maxillofacial environment *via* direct contact. For instance, some restorations may directly contact the gingival tissue, and most endodontic materials are typically in direct contact with the pulp chamber. Moreover, as dental materials become increasingly bioactive and interactive with the oral tissues, a thorough characterization of the biological response is critical.

*Address correspondence to these authors at the Polymers Division, National Institute of Standards and Technology, Gaithersburg, MD 20899-8543, USA; E-mail: nancy.lin@nist.gov, slgibson@nist.gov

A large amount of work has been devoted to improving the clinical performance of dental composites by incorporating new chemistries or improving existing formulations. Multiple chemical and processing parameters have been shown to affect physical and mechanical properties as well as biocompatibility [7]. The matrix alone is typically comprised of a binary or ternary resin mixture in which the material properties can be easily adjusted by chemical and compositional changes and a large number of processing parameters. The addition of the filler phase, typically comprised of different filler types, sizes, shapes, and surface treatments, further complicates the formulation. The filler loading is often determined by the desired application. For example, flowable composites such as those used in dental adhesives are lightly filled. On the other hand, dental restoratives targeted for posterior tooth restorations are more highly filled to withstand greater forces of mastication. Depending on the desired properties, different filler sizes (among other parameters) are selected. Larger fillers generally permit higher filler loading, which in turn increases the composite strength and reduces the overall composite shrinkage. A nano-filler is often incorporated to improve the wear resistance and sometimes to improve the stability of the composite paste. Thus, many of the dental composites commercially available today are dual-filled systems to achieve both high filler loading and enhanced wear resistance [1].

Combinatorial and high throughput (C&HT) methods, which are useful tools in chemistry [8, 9] and biology [10, 11], have become increasingly popular in materials discovery, characterization, and optimization and are ideal for studying complex systems with multiple parameters [12]. Advantages for utilizing combinatorial methods include faster data acquisition, more thorough examination of the

1386-2073/09 $55.00+.00

experimental variables, and reduced experimental errors. For photopolymerized dental polymers and composites, C&HT methods have been employed to determine the degree of conversion, mechanical properties [13], and polymerization shrinkage [14]. We previously developed both the fabrication methods for producing systematically varied dental polymers and the corresponding characterization techniques (test suite) for quantifying several material properties on the same sample. These properties included degree of conversion (DC) quantified by near infrared (NIR) spectroscopy and Fourier transform infrared spectroscopy-reflectance mode, mechanical properties characterized by nanoindentation, and cell response evaluated *via* bioassays modified specifically for combinatorial studies [7, 13, 15]. The results reaffirm that a single optimum composition does not exist and highlight the need to thoroughly test all important properties for each combination of materials and processing parameters.

Our previous study focused on 2-dimensional (2D) composition/degree of conversion gradients of dental polymers using a monomer system consisting of binary mixtures of 2,2-Bis(4-(2-hydroxy-3-methacryloxypropoxy)phenyl)propane (BisGMA) and triethylene glycol dimethacrylate (TEGDMA). For this monomer system, the cell response did not change significantly with the chemical composition but did strongly correlate with DC [7]. Since the monomer composition minimally affected the cell response, a single resin system (BisGMA-TEGDMA in a 50:50 mass ratio) was selected for this study. In the current study, we extend the combinatorial bioassay to dental composites. Gradient samples with variations in filler composition (type and content) and irradiation along orthogonal axes were fabricated and characterized using NIR spectroscopy and confocal microscopy to measure DC and roughness, respectively. RAW 264.7 macrophage-like cells were seeded onto the gradient substrates and cultured for 24 h. Macrophages are involved in the inflammatory response and are likely to be found near the site of a recently placed restoration. The cell response was quantified in terms of cell viability, density, and spreading as a function of position on the composite gradient samples.

MATERIALS AND METHODS

Materials*

BisGMA and TEGDMA were obtained from Esstech, Inc. The photoinitiator system of camphorquinone (CQ) and ethyl 4-*N*,*N*-dimethylaminobenzoate (4E) was purchased from Aldrich Corp. The SP 345 silane glass filler (SG) and fumed amorphous silica filler (OX50) were provided by the L.D. Caulk company. The average diameter for SG and OX50 was 0.70 μm and 0.04 μm, respectively. Methacryloxypropyltrimethoxy-silane (MPTMS) and n-octadecyltrimethoxysilane (OTMS) were purchased from Gelest, Inc. All reagents were used as received. Cell culture reagents were purchased from Invitrogen Corp. unless otherwise noted.

* Certain equipment, instruments or materials are identified in this paper to adequately specify the experimental details. Such identification does not imply recommendation by the National Institute of Standards and Technology, nor does it imply the materials are necessary the best available for the purpose.

Composite Preparation

BisGMA and TEGDMA (mass ratio = 50:50) were activated for blue light photopolymerization with 0.2% CQ and 0.8% 4E (by mass) and stored in the dark until use. The SG and OX50 fillers were hand mixed into the activated resin until uniformly distributed according to the detailed compositions listed in Table **1**. These compositions were selected in order to evaluate both filler type and filler mass ratio.

Table 1. **Composite Formulations**

Composition	Activated Resin (% by mass)	SG (% by Mass)	OX50 (% by Mass)
C1	35	65	0
C2	50	50	0
C3	50	45	5
C4	65	30	5
C5	80	15	5

The gradient specimen consisted of discrete changes in composition along one axis with an orthogonal gradient in methacrylate conversion, which was varied in a continuous fashion (Fig. **1**). The procedures for preparing the composite gradient sample were adapted from those previously used to prepare polymer gradient samples [7, 13]. Briefly, a sandwich mold was prepared using two surface treated glass slides and a poly(dimethylsiloxane) spacer (thickness ≈ 1.5 mm) with 5 channels (3 mm x 60 mm) stamped out. One glass slide was surface treated with MPTMS to enhance adhesion between the dimethacrylate polymer and glass slide while the other slide was surface treated with OTMS to allow easy separation of the polymer and glass. The spacer was placed on the MPTMS treated slide, and the composite mixtures were spread into the separate channels, thus keeping the compositions discrete. The channels were covered with the OTMS treated glass, and the assembly was clamped together and placed 10 cm beneath a light source (Dentsply Triad 2000 replacement Tungsten halogen light bulb 250 W, 120 V). The samples were irradiated for 15 s per side positioned with one edge directly under the center of the light source. The samples were then partially shielded and further exposed for 1 min on each side. All measurements were carried out at least 24 h after light exposure to ensure that the conversion no longer changed significantly with post-cure time. A notch was made across the composition gradient at the high conversion end and was defined as the zero position for subsequent measurements.

NIR Spectroscopy

Transmission NIR spectroscopy was performed using a Nicolet Magna 550 FTIR spectrometer (Madison, WI) configured with a white light source, a CaF_2 beam splitter, and an InSb detector. The NIR spectra in the region of 7000 cm^{-1} to 4000 cm^{-1} were acquired from 32 co-added scans at 6 cm^{-1} resolution. The gradient sample was clamped to a card with a wide opening for the NIR beam and was shifted vertically or horizontally to place the appropriate sample location directly in the beam path. The DC was calculated as the reduction in the methacrylate peak height at 4743 cm^{-1}, with peak height

measurements taken before and after photopolymerization and normalized to an internal aromatic reference peak at 4623 cm^{-1} [13]. Conversion measurements were collected over 50 mm at 10 mm intervals. The relative uncertainty associated with the NIR measurements is 3% and includes the standard deviation, instrument error, and sample variations.

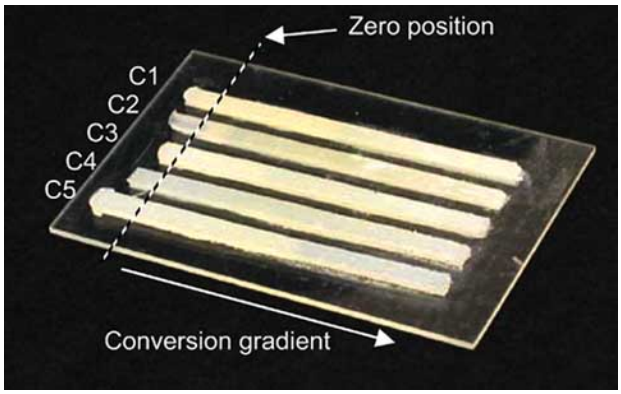

Fig. (1). Photograph of a gradient sample containing five discrete compositions, each with a continuous variation in DC.

Surface Morphology Characterization

A reflection laser scanning confocal microscope (LSCM, laser wavelength = 543 nm) was employed to characterize the surface morphology and RMS (root-mean-square) surface roughness [16, 17]. A 150X and a 50X objective were used to scan an area of 61.4 μm x 61.4 μm and 183.4 μm x 183.4 μm, respectively. LSCM images were prepared as 2D intensity projections of the composite surfaces, in which an image is formed by summing the stack of images over the z direction, 512 pixels x 512 pixels. The resultant 2D projection image is effectively the sum of all the light back-scattered by different layers of the surface as far into the composite as possible. The pixel intensity represents the total amount of back-scattered light, so lighter areas represent regions scattering more light than darker areas. From the 3D topographic profiles, the RMS surface roughness, S_q, was calculated using a surface tilt correlation and an automatic plane fit [17]. Plane fit is commonly used to remove tilt from images. A single polynomial fit was calculated for the entire image and then subtracted from the image. S_q was calculated without a numerical filter according to the following formula:

$$S_q = \sqrt{\frac{1}{N_x \bullet N_y} \bullet \sum_{i=1}^{N_x} \bullet \sum_{j=1}^{N_y} \bullet \left[z(x_i, y_j) - S_c \right]^2} \quad (1)$$

$$S_c = \frac{1}{N_x \bullet N_y} \bullet \sum_{i=1}^{N_x} \bullet \sum_{j=1}^{N_y} \bullet z(x_i, y_j) \quad (2)$$

Here, z (x_i,y_j) is the surface height at position (x_i,y_j), and N_x and N_y are the number of pixels in the X- and Y-directions, respectively.

Cell Culture

The murine RAW 264.7 macrophage-like cell line (American Type Culture Collection, ATCC TIB-71) was cultured in Roswell Park Memorial Institute (RPMI) medium 1640 supplemented with 10% (volume fraction) heat-inactivated fetal bovine serum. Cells were maintained in humidified incubators (5% by volume CO_2, 37 °C).

Cell Seeding

Prior to cell seeding, samples were sterilized using ethylene oxide gas (Anprolene Sterilization System, Andersen Products, Inc.). After degassing for 3 d at room temperature, samples were rinsed and aged in phosphate buffered saline (PBS) at 37 °C to remove toxic leachables. PBS solution was changed on days 1, 3, 5, and 7. On day 7, each sample was transferred to a new dish (OmniTray, Nalge Nunc International), and a suspension of cells in 5 mL growth medium (1.9×10^5 cells/mL) was added to cover each sample. After 15 min, 25 mL growth medium containing 8.7×10^4 cells/mL were added to fill the entire dish, and samples were transferred to the incubator. Control cells were seeded in 6-well tissue culture polystyrene (TCPS) plates (2 mL per well of 1.2×10^5 cells/mL). The seeding density on the gradient samples and on the control TCPS wells was 2.5×10^5 cells/cm^2.

Quantitative Viability Assay

After 24 h, the samples were evaluated for viability using calcein acetoxymethyl ester (calcein AM, live cells), ethidium homodimer-1 (EthD-1, dead cells), and Hoechst 33342 (H33342, all nuclei) as previously described [7]. Briefly, the growth medium was replaced with new growth medium containing 2 μmol/L calcein AM, 2 μmol/L EthD-1, and 10 μmol/L H33342. After 15 min of staining, the samples were transferred to new dishes containing growth medium and imaged using a Leica DMA upright microscope with epifluorescence capabilities, a Hamamatsu digital camera, and Image-Pro Plus software (Media Cybernetics, Inc.). Images were collected over a DC range of 52% DC to 76% DC at intervals of 4% DC. At least 4 separate fields of view were imaged for each DC value using a 10X objective, resulting in a total imaged area greater than 1.4 mm^2 for each location. At least 3 separate gradient samples were imaged for each data set. Cell viability and cell density were quantified using macros written in Image-Pro Plus. The dead cell count was determined by the number of nuclei stained with EthD-1, and the live cell count was the number of nuclei stained with only H33342.

Cell Area Quantification

Samples for measuring cell area were fixed, permeabilized, and stained with 2 μg/mL DAPI and 1 μg/mL Alexa Fluor 488-maleimide in PBS for 1 h. Images were collected as described above, and analysis was performed using Image-Pro Plus macros. Cell density was determined by counting the total number of nuclei per image. Cell area data were recorded for single cells. Cells undergoing mitosis or in contact with other cells (as indicated by the presence of more than one nucleus per object) and cells not fully in the image were excluded from the area analysis [18]. Area measurements were natural log transformed prior to statistical analysis.

Statistical Analysis

Data were analyzed using one-way or two-way analysis of variance (ANOVA), and post hoc analysis was performed

using Fisher's least significant difference (LSD) test with a 95% confidence interval to indicate significant differences ($P < 0.05$). The relative uncertainties associated with the viability, cell density, and cell area measurements are estimated by the error bars on the corresponding figures. Significance of the correlation coefficients for cell area data were evaluated using a t-test and a 95% confidence interval in VassarStats.

RESULTS AND DISCUSSION

The current study used a combinatorial approach to demonstrate that the evaluation of cell response on dental composite materials is complex and involves several material properties and interactions among these properties. Two dimensional gradient samples varying orthogonally in composite formulation and DC were fabricated. The compositions were kept discrete for straightforward gradient fabrication and characterization, whereas DC was varied in a continuous fashion (Fig. **1**). All compositions consisted of the same matrix resin, but varied in the filler type and content (Table **1**). In this study, we examined the *in vitro* cell response to the composites as a function of filler content and type, *i.e.*, macro-filler versus nano-filler. Compositions C1 and C2 contained only macro-filler, whereas compositions C3, C4, and C5 contained 5% (by mass) nano-filler. In addition, compositions C2 and C3 contained the same monomer to filler mass ratio but varied in filler composition.

The DC profile for all five compositions on each gradient sample was characterized using NIR (Fig. **2**). Neither filler type interfered with the NIR region of interest (4743 cm^{-1} for the methacrylate double bond and 4623 cm^{-1} for the aromatic reference peak). Since the same resin mixture was used in all the composite formulations, the NIR spectra for all samples could be compared to the same uncured composite paste and with each other. An ANOVA analysis of DC for all compositions revealed a significant difference in DC with respect to composition (P-value < 0.001, n = 12). The composite with the highest filler loading (C1, Table **1**) consistently showed a lower DC for each position evaluated ($P < 0.05$, except for the 30 mm position) when compared to the other compositions. The lower DC indicated slightly reduced reaction kinetics, which are expected since the increased amount of macro-filler reduces the transmission of the light to the resin. The kinetics were less affected for composites with a filler loading at or below 50% by mass. Since there were variations in DC among the five compositions as well as slight (but not statistically significant) sample-to-sample variations, positions corresponding to predetermined DC values (52%, 56%, 60%, 64%, 68%, 72%, and 76%) were identified for each composition and sample and used for evaluating the cell response.

An interesting observation for the gradient samples was the appearance of the surface along the conversion gradient. Visually, the high conversion end appeared to be highly reflective, and the surface became gradually duller in appearance with decreased DC. The trend was observed for all compositions. In order to better characterize the surface morphology, we examined the surface features using confocal microscopy. Atomic force microscopy (AFM) could not be used for these composite gradients due to the magnitude of the surface roughness, particularly as the DC decreased. Projection images of the surface morphology as a function of position along the conversion gradient (Fig. **3**, top) illustrate that surface roughness increased along the decreasing conversion gradient. The larger images were collected using a 50X objective, and the inset images were collected using a 150X objective for a closer examination of the surface features. The corresponding RMS roughness was calculated from images generated using the 50X objective (Fig. **3**, bottom). All composites showed an increased RMS roughness with decreased DC. We have demonstrated previously that for similar gradient samples prepared from dental monomers without any filler, the surface was relatively smooth and the RMS roughness, as measured using AFM, remained constant along the conversion gradient [15]. Therefore, the roughness gradient appears to result from the polymerization process in the presence of filler particles, although the exact mechanism is unclear at this point.

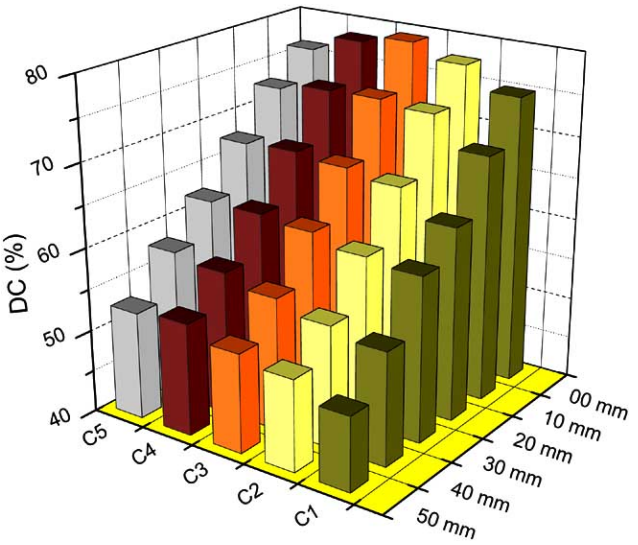

Fig. (2). Degree of conversion as a function of position for compositions varying in filler mass ratio and type. Data are the average of 12 gradient samples. The relative uncertainty associated with these measurements is 3%.

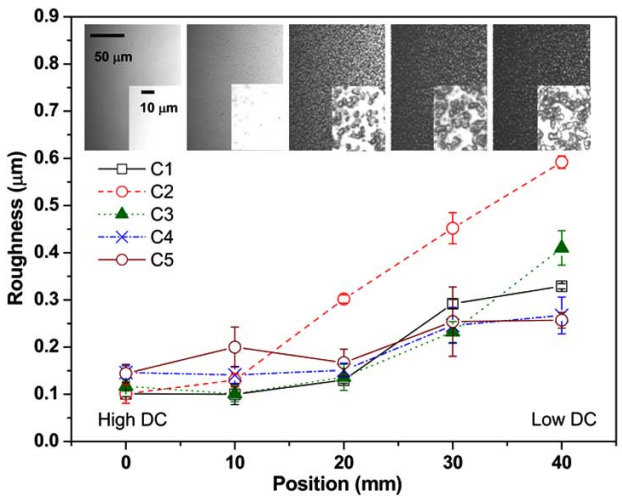

Fig. (3). Composite surface roughness as a function of position for a representative gradient sample. Inset images are shown for composition C2. RMS roughness data points represent the average of three measurements, and error bars represent one standard deviation and are the estimate of standard uncertainty. Lines are drawn to aid the reader's eyes.

RAW 264.7 macrophage-like cells were used to screen the *in vitro* response to the 2D gradient samples. We first examined the cell response in terms of cell viability and density (Fig. **4**). Filler content had a significant effect on cell viability, with increasing filler content reducing the toxicity of the composites (Fig. **4A**). For C1, C2, and C3, the three compositions with highest filler content, cell viability was not significantly affected and remained high throughout the entire DC range (52% to 76%). As the filler content decreased, cell viability was reduced. Compositions C4 and C5 resulted in a significantly reduced viability at conversions below 64% DC. Cell viability on C5 was significantly different ($P < 0.05$) overall when compared to viability on the other compositions. Cell viability results measured as a function of DC for compositions with lower filler loading levels are consistent with those observed for the pure polymer [7]. Since the dimethacrylate phase is likely the primary contributor to cell toxicity, it is reasonable to expect increased cell viability as the dimethacrylate phase decreases and the filler content increases. At higher loading levels, the effect of DC becomes less pronounced as the cells sense more filler particles and an altered surface morphology.

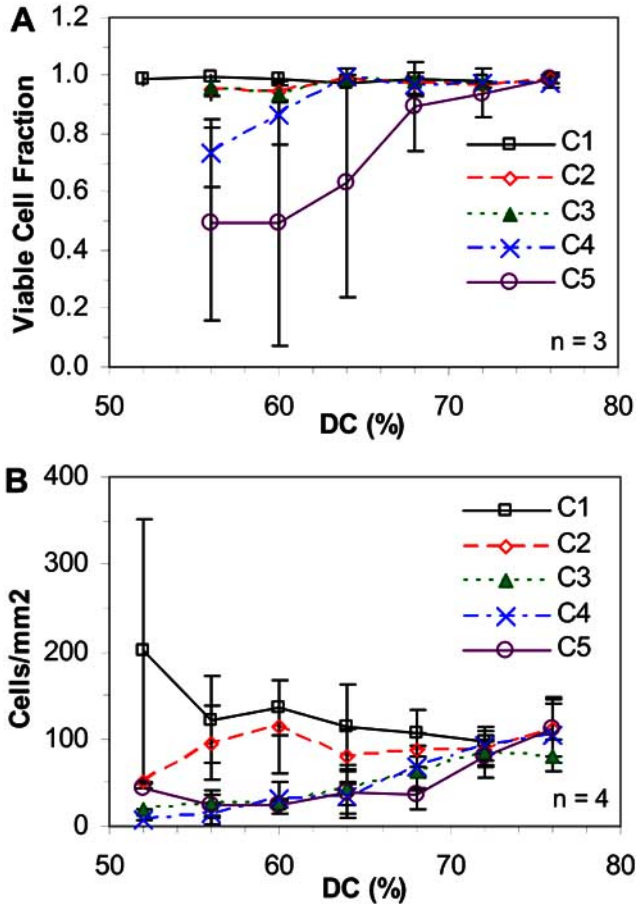

Fig. (4). Macrophage viable cell fraction (**A**) and cell density (**B**) determined as a function of DC and composition. C1 has the highest filler content and C5 has the least amount of filler. Data points represent the average value, and error bars represent one standard deviation and are the estimate of standard uncertainty. Lines are drawn to aid the reader's eyes.

As shown in our previous studies, cell viability alone does not provide an adequate picture of the cell response to a given material. If a material is toxic, it is possible that cells will die and detach from the surface prior to the viability study, inflating the viable fraction as measured using adherent cells. Thus, a second parameter associated the cell response was also evaluated: cell density (Fig. **4B**). In agreement with the viability data, compositions C4 and C5 had a reduced cell density as the DC decreased. Composition C3, which had no significant changes in viability as a function of DC, also showed a reduced cell density at low DC levels. Cell density was significantly reduced below DC levels of 68%, 72%, and 72% for C3, C4, and C5, respectively. Cell density decreased at positions where the DC was relatively high and the cell viability was near 100%, demonstrating that even a slightly reduced DC can have a negative impact on cell adhesion. The highly filled C1 had no significant reduction in cell density as a function of DC. In fact, the trend on C1 revealed a slight increase in cell density as the DC decreased. Compositions C2 and C3 were comprised of the same dimethacrylate to filler ratio, with C3 containing some nano-filler. C3 showed a trend in cell density similar to that of C4 and C5 which also contained nano-filler, where the cell density decreased with decreasing DC. Yet, C2 had no significant changes in cell density as DC decreased. This suggests that the filler type also affects the cell response.

Cell area was quantified as a third indicator of cell response to complement the cell viability and density measurements (Fig. **5**). Overall, cells were more spread at the higher conversions (Fig. **5A**), even on highly filled C1 and C2, which showed no significant changes in cell viability or cell density as a function of DC. The differences in cell area can be viewed by evaluating the distribution of cell area, an example of which is shown for C1 in Fig. (**5B**). The cells at the 52% DC position are less spread than those at 72% DC. The average cell area is plotted as a function of DC for each composition in Fig. (**5C**). Since these data do not have a normal distribution, the area data were natural log transformed to yield a normal distribution prior to statistical analysis. A number of differences were significant with respect to DC and with respect to conversion (Fig. **5D**). For instance, all DC levels on C1 were significantly different with respect to all other DC levels, except 60% and 72%, which were not significantly different. Likewise, in looking at a single conversion level, such as 76%, C5 was significantly different from the other compositions. Overall, cells on many of the compositions had statistically reduced areas at the lower conversions (52%, 56%, 60%) and statistically higher areas at the higher DC levels (72%, 76%). The overall trend in cell area as a function of DC was evaluated for each composition. The significance of the correlation coefficient associated with each best-line fit revealed that compositions C1 and C2 had a significant trend of increasing cell area with increasing DC ($P < 0.05$). Thus, cell area changed even at locations where viability and/or density were unaffected. These data again illustrate the importance of quantifying more than one aspect of the cell response.

The results from this study indicate that for composition C1, which contained the most filler, DC has no significant effect on the cell viability or density within the DC range studied. However, there must be a parameter that resulted in the slight trend of increasing cell number and concurrent, significant reduction in cell area at low DC positions. The increased surface roughness at low DC locations (Fig. **3**)

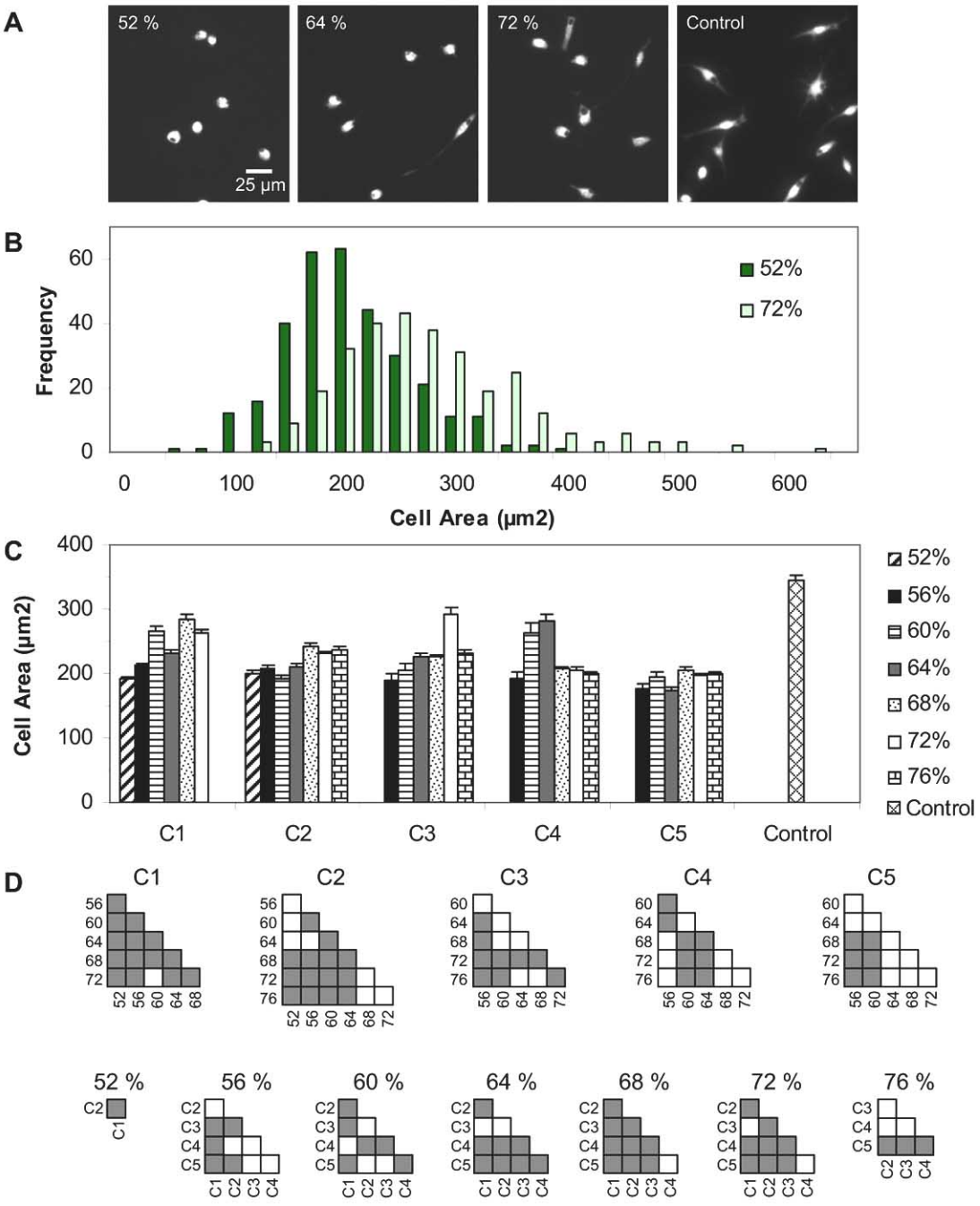

Fig. (5). Effects of composition and DC on macrophage spreading. (**A**) Images of cells (stained with Alexa Fluor 488-maleimide) on composition C1 and on the control tissue culture polystyrene. (**B**) An example histogram showing differences in cell area at 52% and 72% DC on C1. (**C**) Cell area as a function of composition and DC, with data combined from three separate gradient samples (n = 3). Data bars represent the average value, and error bars represent the standard error of the mean (SEM) and are the estimate of standard uncertainty. (**D**) Statistical analysis of cell area for each composition (C1-C5) and DC value (52% - 76%). Shaded boxes indicate significant differences ($P < 0.05$). White boxes indicate a lack of significant difference.

may have led to these trends in cell response on C1. This observation is consistent with previous results that demonstrate varied cell adhesion with increased surface roughness [19, 20]. Likewise, for all compositions, at least four variables affect the cell response: dimethacrylate to filler ratio, filler type and composition, DC, and surface roughness. The complex interplay among these material properties resulted in the varied cell response on the gradient samples.

CONCLUSIONS

Two-dimensional composition and degree of conversion gradient samples were fabricated to screen the effects of

filler type/content and extent of polymerization on macrophage cell response. Three parameters, viable cell fraction, cell density, and cell spreading, were evaluated to assess the overall cell response to the composite substrates. All three parameters of cell response were affected on the gradient samples, with DC, filler type, filler amount, and surface morphology all having significant effects. Cytocompatibility of the composites was found to improve with increasing filler content. Thus, our results indicate that increasing the filler loading of the composites will reduce the toxicity of under-cured polymers, although the best practice remains to achieve a high DC for dimethacrylate polymers. The combinatorial platform presented here provides a method to evaluate a range of composite properties and formulations on a single gradient sample. This method of testing the composites allows for a thorough evaluation of the parameters of interest and the rapid collection of large data sets.

ACKNOWLEDGEMENTS

Financial support was provided through an NIDCR/NIST Interagency Agreement Y1-DE-7005-01. The dental resins and fillers were kindly donated by Esstech, Inc. and Dentsply Caulk, respectively. We would also like to thank Drs. Jirun Sun and Joseph Antonucci for their helpful discussions.

REFERENCES

[1] Ferracane, J. A. *Materials in Dentistry: Principles and Applications;* 2nd ed.; Lippincott Williams & Wilkins: Baltimore, **2001**.

[2] Sarrett, D. C. Clinical challenges and the relevance of materials testing for posterior composite restorations. *Dent. Mater.*, **2005**, *21*(1), 9-20.

[3] Santerre, J. P.; Shajii, L.; Leung, B. W. Relation of dental composite formulations to their degradation and the release of hydrolyzed polymeric-resin-derived products. *Crit. Rev. Oral. Biol. Med.*, **2001**, *12*(2), 136-51.

[4] Geurtsen, W. Biocompatibility of resin-modified filling materials. *Crit. Rev. Oral Biol. Med.*, **2000**, *11*(3), 333-55.

[5] Schweikl, H.; Hiller, K. A.; Bolay, C.; Kreissl, M.; Kreismann, W.; Nusser, A.; Steinhauser, S.; Wieczorek, J.; Vasold, R.; Schmalz, G. Cytotoxic and mutagenic effects of dental composite materials. *Biomaterials*, **2005**, *26*(14), 1713-9.

[6] St John, K. R. Biocompatibility of dental materials. *Dent. Clin. North Am.*, **2007**, *51*(3), 747-60.

[7] Lin, N. J.; Drzal, P. L.; Lin-Gibson, S. Two-dimensional gradient platforms for rapid assessment of dental polymers: a chemical, mechanical and biological evaluation. *Dent. Mater.*, **2007**, *23*(10), 1211-20.

[8] Ugi, I.; Heck, S. The multicomponent reactions and their libraries for natural and preparative chemistry. *Comb. Chem. High Throughput Screen.*, **2001**, *4*(1), 1-34.

[9] Sun, C. M. Recent advances in liquid-phase combinatorial chemistry. *Comb. Chem. High Throughput Screen.*, **1999**, *2*(6), 299-318.

[10] Masimirembwa, C. M.; Thompson, R.; Andersson, T. B. *In vitro* high throughput screening of compounds for favorable metabolic properties in drug discovery. *Comb. Chem. High Throughput Screen.*, **2001**, *4*(3), 245-63.

[11] Panicker, R. C.; Huang, X.; Yao, S. Q. Recent advances in peptide-based microarray technologies. *Comb. Chem. High Throughput Screen.*, **2004**, *7*(6), 547-56.

[12] Amis, E. J. Reaching beyond discovery. *Nat. Mater.*, **2004**, *3*(2), 83-5.

[13] Lin-Gibson, S.; Landis, F. A.; Drzal, P. L. Combinatorial investigation of the structure-properties characterization of photopolymerized dimethacrylate networks. *Biomaterials*, **2006**, *27*(9), 1711-7.

[14] Barnes, S. E.; Cygan, Z. T.; Yates, J. K.; Beers, K. L.; Amis, E. J. Raman spectroscopic monitoring of droplet polymerization in a microfluidic device. *Analyst*, **2006**, *131*(9), 1027-33.

[15] Lin, N. J.; Bailey, L. O.; Becker, M. L.; Washburn, N. R.; Henderson, L. A. Macrophage response to methacrylate conversion using a gradient approach. *Acta Biomater.*, **2007**, *3*(2), 163-73.

[16] Corle, T. R.; Kino, G. S. *Confocal Scanning Optical Microscopy and Related Imaging Systems;* Academic Press: San Diego, **1996**.

[17] Sung, L. P.; Jasmin, J.; Gu, X. H.; Nguyen, T.; Martin, J. W. Use of laser scanning confocal microscopy for characterizing changes in film thickness and local surface morphology of UV-exposed polymer coatings. *J. Coat. Technol. Res.*, **2004**, *1*(4), 267-76.

[18] Kennedy, S. B.; Washburn, N. R.; Simon, C. G., Jr.; Amis, E. J. Combinatorial screen of the effect of surface energy on fibronectin-mediated osteoblast adhesion, spreading and proliferation. *Biomaterials*, **2006**, *27*(20), 3817-24.

[19] Zinger, O.; Zhao, G.; Schwartz, Z.; Simpson, J.; Wieland, M.; Landolt, D.; Boyan, B. Differential regulation of osteoblasts by substrate microstructural features. *Biomaterials*, **2005**, *26*(14), 1837-47.

[20] Washburn, N. R.; Yamada, K. M.; Simon, C. G., Jr.; Kennedy, S. B.; Amis, E. J. High-throughput investigation of osteoblast response to polymer crystallinity: influence of nanometer-scale roughness on proliferation. *Biomaterials*, **2004**, *25*(7-8), 1215-24.

Received: August 30, 2007 **Revised: November 5, 2007** **Accepted: May 25, 2008**